Proceedings of the
International Conference on Mechanical Engineering 2003
(ICME2003) 26- 28 December 2003, Dhaka, Bangladesh

ICME03-AM-41

EFFECT OF NONHOMOGENEITY ON THE STRESS INTENSITY FACTOR FOR EDGE CRACKS IN AN FGM CYLINDER

A. M. Afsar, M. Anisuzzaman and M. A. Motaleb

Department of Mechanical Engineering, Bangladesh University of Engineering and Technology
Dhaka 1000, Bangladesh

ABSTRACT

This study deals with a thick-walled functionally graded material (FGM) circular cylinder subjected to an internal pressure. Two cases of crack orientation *viz*. a single radial edge crack and two diametrically opposed edge cracks emanating from the inner surface of the cylinder are considered. The incompatible eigenstrain induced in the cylinder material after cooling from sintering temperature due to nonuniform coefficient of thermal expansion is taken into account. The nonhomogeneity of the cylinder material is simulated by a distribution of equivalent eigenstrain and the problem is thus reduced to the solution of the crack problem of a homogenized cylinder with incompatible and equivalent eigenstrains under an internal pressure. Representing the cracks by a continuous distribution of edge dislocations and using their complex potential functions, a singular integral equation is formulated, which is solved numerically to calculate stress intensity factors. Numerical results are obtained for a TiC/Al_2O_3 FGM cylinder for different types of material distribution. It is revealed that the stress intensity factors are substantially dependent on the material nonhomogeneity of the FGM cylinder and can be controlled by choosing an appropriate material distribution.

Keywords: Functionally graded material, Micromechanics, Stress intensity factor, Eigenstrain, Edge dislocation.

1. INTRODUCTION

Functionally graded materials (FGMs) consist of two or more distinct material phases, such as different ceramics or ceramics and metals. The distribution of each material changes continuously with space variables, which introduces nonhomogeneity in the material. The nonhomogeneity depends on the material distribution that significantly affects both the thermal and mechanical characteristics of these materials. So far, many researchers have paid attention to investigate the effects of material distribution on the characteristics of these materials under various loading conditions and for various geometries. Ootao et al. [1] considered an FGM hollow sphere for thermal stress relaxation by optimization of material distribution. They [2] also considered an FGM hollow cylinder and optimized material distribution for thermal stress relaxation. Analyses of crack problems of these materials are also carried out with a view to investigating the fracture characteristics versus material distribution. Gu and Assaro [3] considered a semi-infinite crack in a strip of an isotropic, functionally graded material under edge loading and in-plane deformation conditions. Afsar and Sekine [4] dealt with the inverse problems of calculating material distributions for prescribed apparent fracture toughness in FGM coatings around a circular hole in infinite elastic media. They also considered semi-infinite FGM media with a single [5] and periodic [6] edge cracks and computed material distribution profiles for improved fracture characteristics. In another work [7], they calculated optimum material distributions in a thick-walled FGM circular pipe with a single radial edge crack for desired apparent fracture toughness.

From the analyses of homogeneous cylinder, it is found that two diametrically-opposed edge cracks represent the worst geometry of multiple cracking. This motivates the authors of this paper to consider an FGM cylinder for investigating the effect of material nonhomogeneity arising from non-uniform material distribution on the stress intensity factor. In this paper, two crack orientation *viz.* a single radial edge crack and two diametrically-opposed edge cracks emanating from the inner surface of the FGM cylinder are considered. The cylinder is subjected to internal pressure. The incompatible eigenstrain induced in the material due to non-uniform coefficient of thermal expansion as a result of cooling from sintering temperature is also taken into account.

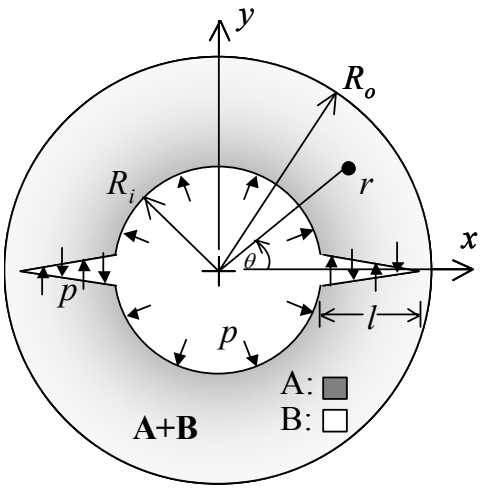

Fig. 1 Analytical model of a thick-walled FGM cylinder

2. MODELING OF THE PROBLEM

The analytical model of the problem is shown in Fig. 1. The Cartesian coordinate system x-y and the polar coordinate system r-θ have the same origin at the center of the cylinder. The inner and outer radii of the cylinder are designated by R_i and R_o, respectively. The constituent materials of the cylinder are A and B which are represented by the black and white colors, respectively. The volume fractions of the constituent materials A and B are denoted by V_A and V_B, respectively. Also, shown in Fig. 1 are two diametrically-opposed edge cracks of equal length l. Along with the inner surface of the cylinder, the crack surfaces are subjected to internal pressure p. It is assumed that the distribution of each constituent material varies with the radial distance r only. When such a cylinder is cooled from sintering temperature, an incompatible eigenstrain ε^* is induced in the material, which is also a function of r only and is given by

$$\varepsilon^* = -\alpha \Delta T \,, \tag{1}$$

where α is the coefficient of thermal expansion which is a function of r only and ΔT is the difference between sintering and room temperatures.

For this model of the cylinder, the effect of material distribution on the stress intensity factor is investigated.

3. STRESS INTENSITY FACTOR

3.1 Approximation Method of Stress Intensity Factors

The presence of nonhomogeneity in FGMs complicates the analytical study of fracture characteristics of these materials due to some mathematical difficulties. Therefore, an approximation method [5] is adopted to calculate stress intensity factor for cracks in the FGM cylinder. According to the approximation method, the FGM cylinder is first homogenized by simulating the material nonhomogeneities by a distribution of equivalent eigenstrain. The distribution of equivalent eigenstrain is such that the elastic fields in both the FGM and homogenized cylinders are identical for the same loading condition. Then a method is formulated to calculate the stress intensity factor for the crack in the homogenized cylinder. Since the equivalent eigenstrain is determined from the condition of identical elastic fields in the uncracked FGM and homogenized cylinders, the elastic field in the cracked homogenized cylinder cannot exactly represent the elastic field in the cracked FGM cylinder. Consequently, the stress intensity factors calculated for a crack in the homogenized cylinder with the equivalent eigenstrain represent the approximate values of stress intensity factors for the same crack in the FGM cylinder.

3.2 Equivalent Eigenstrain for Homogenization

As stated earlier, the equivalent eigenstrain to homogenize the FGM cylinder is determined from the condition of identical elastic fields in the FGM and homogenized cylinders. However, there is no straightforward method to determine the elastic field in FGM cylinder. Therefore, an alternate approach [7] is adopted for this purpose. The FGM cylinder is radially divided into layers of infinitesimal thickness as shown in Fig. 2, which shows one half of the cylinder. Each layer is assumed to have constant material properties but differ from the other layers. The inner and outer radii of the ith layer are, respectively, denoted by r_{i-1} and r_i, where $r_0 = R_i$ and $r_n = R_o$. The pressures at the inner and the outer surfaces of the ith layer are, respectively, P_{i-1}^f and P_i^f which are the resultant of pressures due to the applied internal pressure p and the incompatible eigenstrain ε_i^* in the ith layer. For this layered FGM cylinder, the stress field is given in Ref. [8].

Now we consider a homogeneous cylinder having the same geometry and determine the elastic field due to the same applied internal pressure p and incompatible eigenstrain following the same techniques as the layered FGM cylinder. Here, it is noted that the material properties are same for all the layers. The elastic field for such a cylinder is given in Ref. [8]. Another elastic field

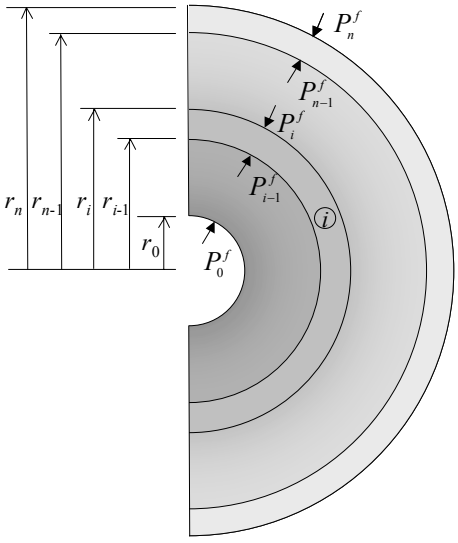

Fig. 2 Layered FGM cylinder

in the homogeneous cylinder is determined due to equivalent eigenstrain. By principle of superposition, the resultant elastic field in the homogeneous cylinder is then obtained. Equating the elastic fields in the FGM and homogeneous cylinders, one can obtain the distribution of equivalent eigenstrain as

$$\varepsilon_{r,e}^{i}=\frac{(1+\nu_i)(1-2\nu_i)}{E_i(1-c_i^2)}\left[(c_i^2P_{i-1}^f-P_i^f)-\frac{c_i^2}{1-2\nu_i}\frac{r_i^2}{r^2}(P_{i-1}^f-P_i^f)\right]$$
$$-\frac{(1+\nu_0)(1-2\nu_0)}{E_0(1-c_i^2)}\left[(c_i^2P_{i-1}^h-P_i^h)-\frac{c_i^2}{1-2\nu_0}\frac{r_i^2}{r^2}(P_{i-1}^h-P_i^h)\right]$$
$$+\frac{1}{E_0(1-c_i^2)}\left[c_i^2\left(1-\frac{r_i^2}{r^2}\right)(P_{i-1}^h-P_{i-1}^f)-\left(1-c_i^2\frac{r_i^2}{r^2}\right)(P_i^h-P_i^f)\right]$$
$$-\frac{\nu_0}{E_0(1-c_i^2)}\left[c_i^2\left(1+\frac{r_i^2}{r^2}\right)(P_{i-1}^h-P_{i-1}^f)-\left(1+c_i^2\frac{r_i^2}{r^2}\right)(P_i^h-P_i^f)\right]$$
$$-\frac{2\nu_0}{E_0(1-c_i^2)}\left[\nu_0(c_i^2P_{i-1}^h-P_i^h)-\nu_i(c_i^2P_{i-1}^f-P_i^f)\right]$$
$$+\frac{\varepsilon_i^*}{E_0}(E_0\nu_i-E_i\nu_0), \qquad (2a)$$

$$\varepsilon_{\theta,e}^{i}=\frac{(1+\nu_i)(1-2\nu_i)}{E_i(1-c_i^2)}\left[(c_i^2P_{i-1}^f-P_i^f)+\frac{c_i^2}{1-2\nu_i}\frac{r_i^2}{r^2}(P_{i-1}^f-P_i^f)\right]$$
$$-\frac{(1+\nu_0)(1-2\nu_0)}{E_0(1-c_i^2)}\left[(c_i^2P_{i-1}^h-P_i^h)+\frac{c_i^2}{1-2\nu_0}\frac{r_i^2}{r^2}(P_{i-1}^h-P_i^h)\right]$$
$$+\frac{1}{E_0(1-c_i^2)}\left[c_i^2\left(1+\frac{r_i^2}{r^2}\right)(P_{i-1}^h-P_{i-1}^f)-\left(1+c_i^2\frac{r_i^2}{r^2}\right)(P_i^h-P_i^f)\right]$$
$$-\frac{\nu_0}{E_0(1-c_i^2)}\left[c_i^2\left(1-\frac{r_i^2}{r^2}\right)(P_{i-1}^h-P_{i-1}^f)-\left(1-c_i^2\frac{r_i^2}{r^2}\right)(P_i^h-P_i^f)\right]$$
$$-\frac{2\nu_0}{E_0(1-c_i^2)}\left[\nu_0(c_i^2P_{i-1}^h-P_i^h)-\nu_i(c_i^2P_{i-1}^f-P_i^f)\right]$$
$$+\frac{\varepsilon_i^*}{E_0}(E_0\nu_i-E_i\nu_0), \qquad (2b)$$

$$\varepsilon_{z,e}^{i}=\frac{2}{E_0(1-c_i^2)}\left[\nu_0(c_i^2P_{i-1}^h-P_i^h)-\nu_i(c_i^2P_{i-1}^f-P_i^f)\right]$$
$$-\frac{2\nu_0}{E_0(1-c_i^2)}\left[c_i^2(P_{i-1}^h-P_{i-1}^f)-(P_i^h-P_i^f)\right]+\frac{\varepsilon_i^*}{E_0}(E_i-E_0). \qquad (2c)$$

The effective properties E_i, ν_i, and α_i of theFGM cylinder are determined by using the mixture rule given by Nan et al. [9].

For the next of the analysis, the FGM cylinder can be replaced by the homogeneous cylinder (referred to as homogenized cylinder) of the same geometry if the equivalent eigenstrain in Eq. (2) is considered along with other loading. The equivalent eigenstrain in Eq. (2) and the incompatible eigenstrain ε_i^* are piecewise continuous. Their continuous distributions for the entire wall thickness of the non-layered homogenized cylinder are obtained by spline interpolation. Finally, the resultant stress field for the non-layered homogenized cylinder for the continuous distributions of equivalent and incompatible eigenstrains is derived [8]. The circumferential stress component of this stress field is given by

$$\sigma_\theta^h=\frac{R_i^2p}{R_o^2-R_i^2}\left[1+\frac{R_o^2}{r^2}\right]+\frac{E_0}{1-\nu_0}\left[-\varepsilon^*+\frac{1}{r^2}\int_{R_i}^{r}r\varepsilon^*dr\right.$$
$$\left.+\left(1+\frac{R_i^2}{r^2}\right)\frac{1}{R_o^2-R_i^2}\int_{R_i}^{R_o}r\varepsilon^*dr\right]$$
$$+\frac{E_0}{2(1-\nu_0^2)}\left[-2(\varepsilon_\theta^e+\nu_0\varepsilon_z^e)+\frac{1}{r^2}\int_{R_i}^{r}r(\varepsilon_r^e+\varepsilon_\theta^e+2\nu_0\varepsilon_z^e)dr\right.$$
$$\left.+\int_{R_i}^{r}\frac{1}{r}(\varepsilon_r^e-\varepsilon_\theta^e)dr+C\left\{1+\frac{R_i^2}{r^2}\right\}\right], \qquad (3a)$$

where

$$C=\frac{1}{R_o^2-R_i^2}\left\{\int_{R_i}^{R_o}r(\varepsilon_r^e+\varepsilon_\theta^e+2\nu_0\varepsilon_z^e)dr-R_o^2\int_{R_i}^{R_o}\frac{1}{r}(\varepsilon_r^e-\varepsilon_\theta^e)dr\right\}. \qquad (3b)$$

3.3 Numerical Formulation for Stress Intensity Factor

Now we consider two diametrically-opposed edge cracks in the homogenized cylinder as shown in Fig.3. Along with the internal pressure p, the incompatible and equivalent eigenstrains are considered. Therefore, the stress intensity factor for these cracks represents the approximate value of the stress intensity factor for the same crack in the FGM cylinder.

The stress field in Eq. (3a) derived for the uncracked homogenized cylinder is disturbed due to the presence of cracks. The redistribution of stress is calculated representing the cracks by a continuous distribution of edge dislocations. By satisfying the boundary conditions along the crack surfaces, the following singular integral equation is derived [8]

$$\frac{2\mu_0}{\pi(\kappa_0+1)}\int_0^l\left[\frac{1}{r-h}+g_1(r,h)+g_2(r,h)\right]b_1(s)ds$$
$$=-p\left[S_f\frac{\sigma_\theta^h}{\sigma_u}+1\right];R_i\le r\le R_i+l,\theta=0, \qquad (4)$$

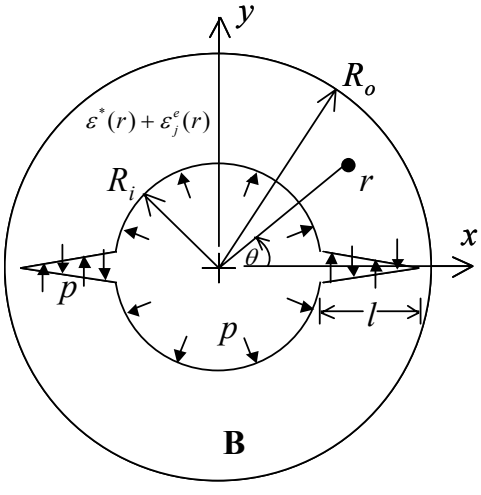

Fig. 3 Cracks in homogenized cylinder

Table 1 Material properties of TiC and Al_2O_3

Material	Young's Modulus (GPa)	Shear Modulus (GPa)	Poisson's Ratio	CTE (/°C)
TiC	462	194	0.19	7.4×10^{-6}
Al_2O_3	380	151	0.26	8.0×10^{-6}

where S_f is the strength factor defined by the ratio of the ultimate strength σ_u of the base material B to the applied internal pressure p.

Using Gauss-Jacobi integral formula, Eq. (4) is converted to a system of linear algebraic equations to solve for $\varphi(T_j)$ as

$$\frac{2\mu_0}{(\kappa_0+1)}\left[\sum_{j=1}^{N}\varphi(T_j)(1+T_j)\left\{\frac{1}{H_i-T_j}+G_1(H_i,T_j)+G_2(H_i,T_j)\right\}\right]=-\frac{2N+1}{2}p\left[S_f\frac{\sigma_\theta^h(H_i)}{\sigma_u}+1\right]. \quad (5)$$

Here, the collocation and integration points are given by

$$H_i=\cos\left(\frac{2i\pi}{2N+1}\right),\ i=1,2,3,.....,N, \quad (6a)$$

$$T_j=\cos\left(\frac{2j-1}{2N+1}\pi\right),\ j=1,2,3,.....,N. \quad (6b)$$

It can be shown that the stress intensity factor is [10]

$$K_I=\sqrt{\pi l}\,\frac{2\mu_0}{(\kappa_0+1)}\sqrt{2}\varphi(+1), \quad (7)$$

where $\varphi(+1)$ is computed from Krenk's [11] interpolation formula

$$\varphi(+1)=\frac{2}{2N+1}\sum_{j=1}^{N}\frac{\sin\left(\frac{2j-1}{2N+1}N\pi\right)}{\tan\left(\frac{2j-1}{2N+1}\frac{\pi}{2}\right)}\varphi(T_j). \quad (8)$$

By using Eqs. (5)-(8), one can readily calculate the stress intensity factor. Here, it is noted that the stress intensity factor for a single radial edge crack can be calculated by setting $G_2(H_i, T_j)$ equal to zero.

4. RESULTS AND DISCUSSION

In order to present some numerical results, we consider a TiC/Al_2O_3 FGM cylinder in which TiC and Al_2O_3 represent the material A and B, respectively. The difference between sintering and room temperatures is taken as 1000°C while the number of layers of infinitesimal thickness is taken as 50 in the numerical calculation. The material properties of TiC and Al_2O_3 are shown in Table 1.

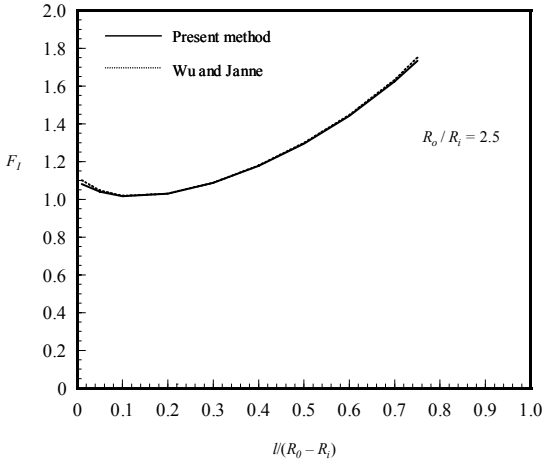

Fig. 4 Comparison of normalized stress intensity factors for a homogeneous cylinder

The method developed for calculating stress intensity factors for two diametrically-opposed edge cracks emanating from the inner surface of the FGM cylinder is first verified by applying it to a homogeneous cylinder. By setting V_A = zero or uniform distribution throughout the wall thickness of FGM cylinder, one obtains a homogeneous cylinder. The stress intensity factor K_I is calculated for such a homogeneous cylinder for R_o/R_i = 2.5. The normalized stress intensity factor $F_I=K_I(1-R_i^2/R_o^2)/2p\sqrt{\pi l}$ is compared with that available in literatures as shown in Fig. 4. The solid line represents the results obtained by the present method while the dotted line the results obtained by Wu and Janne [12]. It is noted that the results obtained by the present method agree well with those obtained by Wu and Janne for the entire range of normalized crack length $l/(R_o-R_i)$.

In order to investigate the effect of nonhomogeneity, three different profiles of material distribution in the FGM cylinder are considered as shown by the curves I, II

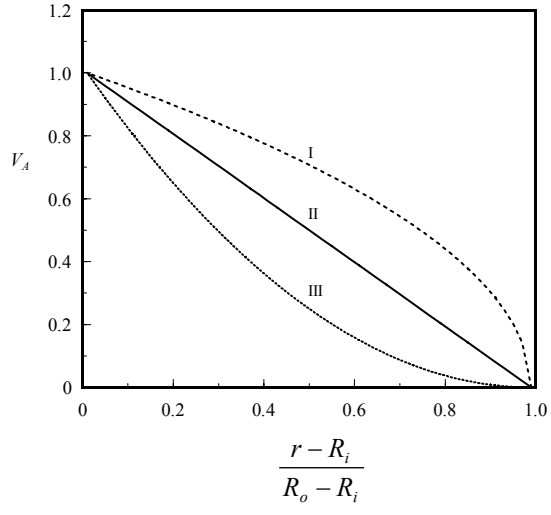

Fig. 5 Prescribed material distributions in FGM cylinder

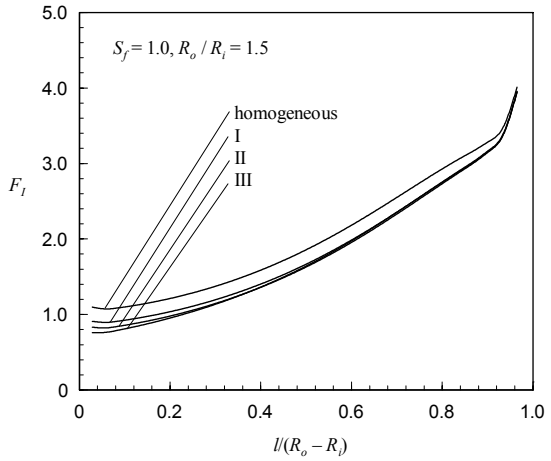

Fig. 6 Effect of nonhomogeneity on stress intensity factors

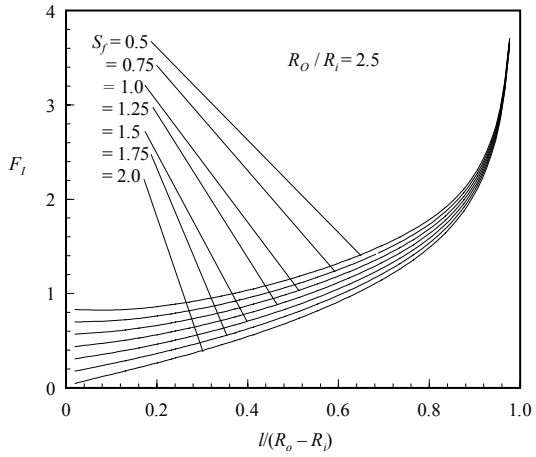

Fig. 8 Effect of strength factor on stress intensity factors

and III in Fig. 5. For these prescribed material distributions and $R_o/R_i = 1.5$, $S_f = 1.0$, normalized stress intensity factor F_I versus normalized crack length $l/(R_o - R_i)$ is plotted in Fig. 6. The results for a homogeneous cylinder are also plotted in the same figure. Note that the stress intensity factor for the homogeneous cylinder is higher than those for FGM cylinders. Further, among the three distributions, the stress intensity factor for material distribution III is minimum for lower range of crack length as the gradient is higher for this distribution near the inner surface of the cylinder.

Figure 7 exhibits the stress intensity factors as a function of the wall thickness of the FGM cylinders. The stress intensity factors are obtained for linear distribution II in Fig. 5. As the wall thickness increases, the stress intensity factor decreases.

The effects of strength factor S_f on the stress intensity factor are also examined and shown in Fig. 8. The results correspond to linear material distribution II in Fig. 5 and $R_o/R_i = 2.5$. The stress intensity factor decreases as the strength factor increases.

A comparison between the stress intensity factors for a single radial edge crack and two diametrically-opposed edge cracks is depicted in Fig. 9. The results are obtained for $S_f = 1.0$ and $R_o/R_i = 2.5$. Note that the stress intensity factor is higher in the case of two diametrically-opposed cracks for any material distribution.

5. CONCLUSIONS

The effect of nonhomogeneity on the stress intensity factor for a single radial edge crack and two diametrically-opposed edge cracks in an FGM cylinder is investigated in this study. It is noted that the stress intensity factor is dependent on the material nonhomogeneity *i.e.* the material distribution in the FGM cylinder. The following salient points can be noted from the numerical results:

i. The stress intensity factors for FGM cylinder are lower than that for a homogeneous cylinder.
ii. The stress intensity factors for an FGM cylinder depend on the material distribution. The stress intensity factor is lower for the material

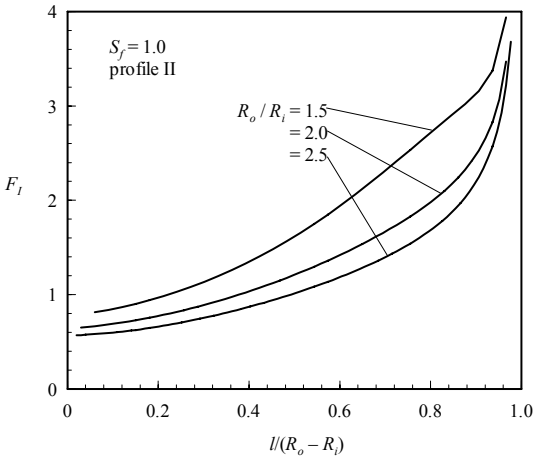

Fig. 7 Effect of wall thickness on stress intensity factors

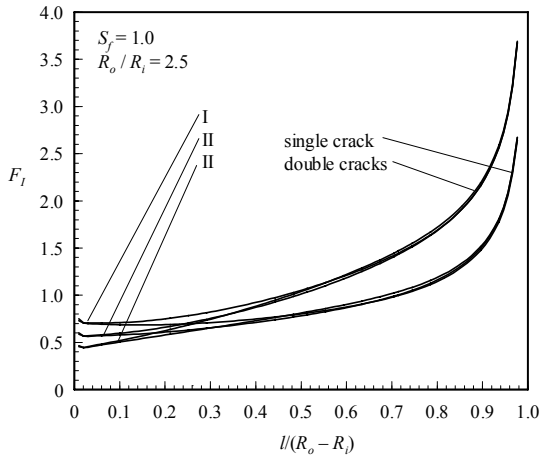

Fig. 9 Comparison of stress intensity factors for a single and two diametrically-opposed cracks

distribution with higher gradient.

iii. The wall thickness of the cylinder and the strength factor have the reverse effect on the stress intensity factors, *i.e.* as the wall thickness and strength factor increase, the stress intensity factors decrease.

iv. Like a homogeneous cylinder, two diametrically-opposed edge cracks are more critical than a single radial edge crack in an FGM cylinder.

6. REFERENCES

1. Ootao, Y., Kawamura, R., Tanigawa, Y. and Imamura, R., 1999, "Optimization of Material Composition of Nonhomogeneous Hollow Sphere for Thermal Stress Relaxation Making Use of Neural Network", Computer Methods in Applied Mechanics and Engineering, 180:185-201.
2. Ootao, Y., Kawamura, R., Tanigawa, Y. and Imamura, R., 1999, "Optimization of Material Composition of Nonhomogeneous Hollow Circular Cylinder for Thermal Stress Relaxation Making Use of Neural Network", Thermal Stresses, 22:1-22.
3. Gu, P. and Assaro, R. J., 1997, "Cracks in Functionally Graded Materials", International Journal of Solids and Structures, 34:1-17.
4. Afsar, A. M. and Sekine, H., 2002, "Inverse Problems of Materials Distributions for Prescribed Apparent Fracture Toughness in FGM coatings Around a Circular Hole in Infinite Elastic Media", Composite Science and Technology, 62:1063-1077.
5. Sekine, H. and Afsar, A. M., 1999, "Composition Profile for Improving the Brittle Fracture Characteristics in Semi-Infinite Functionally Graded Materials", JSME International Journal, Series A, 42:592-600.
6. Afsar, A. M. and Sekine, H., 2000, "Crack Spacing Effect on the Brittle Fracture Characteristics of Semi-Infinite Functionally Graded Materials with Periodic Edge Cracks", International Journal of Fracture, 102(3):L61-L66.
7. Afsar, A. M. and Sekine, H., 2001, "Optimum Material Distributions for Prescribed Apparent Fracture Toughness in Thick-Walled FGM Circular Pipe", International Journal of Pressure Vessels and Piping, 78:471-484.
8. Anisuzzaman, M., 2003, "Brittle Fracture Characteristics of Thick-Walled Functionally Graded Material Cylinders", M. Sc. Dissertation, Mech. Engg. Dept., BUET.
9. Nan, C.-W., Yuan, R.-Z. and Zhang, L.-M., 1993, "The Physics of Metal/Ceramic Functionally Gradient Materials", Ceramic Transaction: Functionally Gradient Materials, Edited by J. B. Holt et al., American Ceramic Society, Westerville, Oh, 34:75-82.
10. Hills, D. A., Kelly, P. A., Dai, D. N. and Korsunsky, A. M., 1996, "Solution of Crack Problems: The Distributed Dislocation Technique", Kluwer Academic Publishers.
11. Krenk, S., 1975, "On the Use of the Interpolation Polynomial for Solution of Singular Integral Equation", Quarterly of Applied Mathematics, 32:479-484.
12. Wu, X.-R. and Janne, A., 1991, "Weight Functions and Stress Intensity Factors Solutions", Pergamon Press PIC, Headington Hill, Oxford OX3OBW, England.